



Synthesis and characterization of trifluoromethylated poly(ether–imidazole–imide)s based on unsymmetrical diamine bearing carbazole and imidazole chromophores in ionic liquids: Study of electrochemical properties by using nanocomposite electrode

Mousa Ghaemy*, Marjan Hassanzadeh, Mehdi Taghavi, Seyed Mojtaba Amini Nasab

Polymer Chemistry Research Laboratory, Department of Chemistry, University of Mazandaran, Babolsar 47416-95447, Islamic Republic of Iran

ARTICLE INFO

Article history:

Received 6 February 2012
Received in revised form 9 June 2012
Accepted 12 June 2012
Available online 26 June 2012

Keywords:

Ionic liquids
Trifluoromethylated polyimides
Solubility
Nanocomposite
Electrochemical oxidation
Thermal properties

ABSTRACT

A novel aromatic trifluoromethylated diamine containing various functional groups was synthesized and characterized by using different spectroscopic techniques. The diamine was polymerized with various dianhydrides in a green media of ionic liquid (IL) without using NMP–pyridine–acetic anhydride. The poly(ether–imidazole–imide) (PEII)s were obtained in good yields (80–96%) with moderate viscosity (0.33–0.67 dL g⁻¹) in a shorter reaction time (10 h vs. 36 h) in IL. The resulting polymers were fully characterized and their properties such as solubility, viscosity, crystallinity, thermal, photophysical, and electrochemical behavior were investigated. They were amorphous and showed excellent solubility even in common organic solvents, such as chloroform and *m*-cresol, with ability to form tough and flexible films. The films were colorless and exhibited high optical transparency, with the UV cutoff wavelength in the range 304–337 nm and the wavelength of 80% transparency in the range 375–400 nm. Furthermore, they also possessed good thermal and thermo-oxidative stability with 10% weight loss temperatures ($T_{10\%}$) in the range 441–528 °C in N₂ atmosphere and in the range 382–494 °C in air. The glass transition temperatures of all polyimides are in the range 204–302 °C.

Their electrochemical behavior was also studied by using adsorptive stripping cyclic voltammetry and impedance spectroscopy on the multi-walled carbon nanotube-modified glassy carbon electrode.

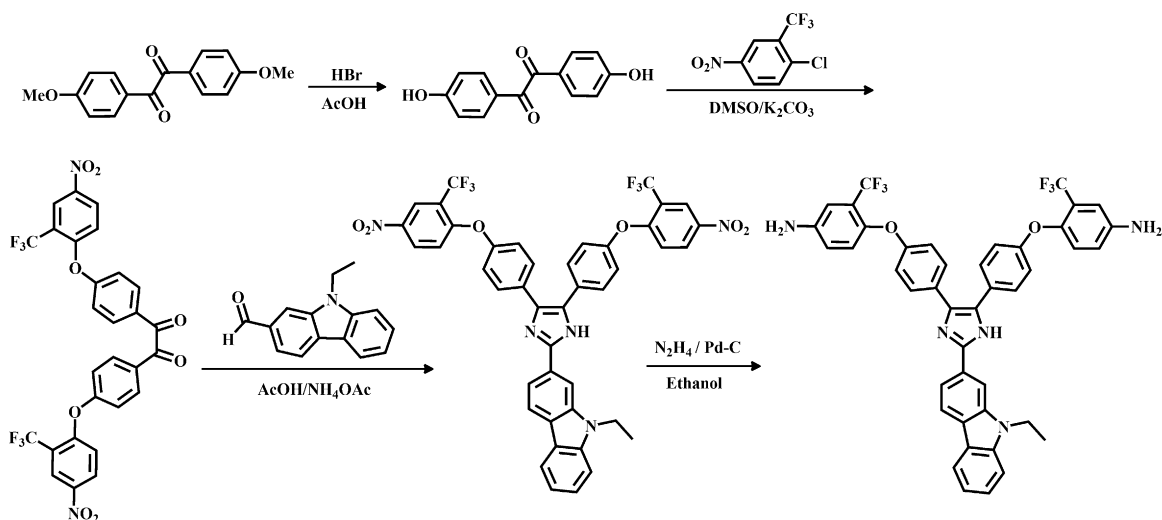
© 2012 Elsevier B.V. All rights reserved.

1. Introduction

Recently many organic synthesis and polycondensation reactions were carried out in room temperature ionic liquids (ILs) as an alternative to many volatile organic solvents [1–4]. There is a need in industry for the replacement of a large amount of toxic solvents with eco-friendly and nonvolatile solvents for the preparation of polyimides (PIs). Imidazolium based ILs have attracted considerable commercial applications in phase transfer catalysis, electrochemistry, extraction, polymerization, and as substitutes for common volatile organic solvents [5–7]. The “green solvents” aspects of ILs are derived mainly from their negligible vapor pressure, non-volatility and inflammability [8–10]. Aromatic PIs constitute an important class of materials because of their many desirable physicochemical and mechanical characteristics, such as good thermal and hydrolytic stability, excellent mechanical strength, low dielectric constant, wear

resistance, and surface inertness [11–13]. During the past decade, interests in these polymers have risen in response to increasing technological applications in a variety of fields such as aerospace, automobile, and microelectronics. However, their applications have been limited in some fields because of their insolubility in common organic solvents and high melting points. Solubility of the PIs has been targeted by several methods, such as introduction of flexible linkage, bulky units in the polymer backbone, bulky pendent substituents, or noncoplanar moieties. Among these approaches, introduction of bulky pendants and heteroaromatic rings into the polymer chains has provided not only enhanced solubility but also good thermal stability and processability [14–21]. There are reports of using imidazole and carbazole rings and their derivatives into polymeric frameworks to improve the solubility of the polymers, which have also been suggested as promising photoconductive and photorefractive materials [22–24]. PIs containing hexafluoroisopropylidene or trifluoromethyl groups are of special interest due to enhanced solubility and optical transparency together with a lower dielectric constant which were attributed to low polarizability of the C–F bond and increasing free volume. The trifluoromethylated PIs also provided

* Corresponding author. Tel.: +98 112 534 2353; fax: +98 112 534 2302.
E-mail address: ghaemy@umz.ac.ir (M. Ghaemy).



Scheme 1. Synthesis of target diamine.

other merits such as good thermal and low moisture absorption [25–27].

Carbon nanotubes (CNTs) with high stiffness and tensile strength have received enormous attention for the composites with desired mechanical properties [28], and also in electrochemistry mainly due to their electrocatalytic effects and ability to promote electron transfer reactions [29]. The modification of electrode substrates with CNTs for use in analytical sensing provides better surface property and more enhanced sensitivity due to excellent chemical and electrical properties of CNTs. Electrochemical oxidation of polymers in various conditions can be a pattern of their stability. The polymer stability is estimated by its potential of oxidation. By using electrochemical studies, the determinant bonds in the polymer structures, which are responsible for polymer oxidation, can be recognized and the ability of different monomer structures on polymer stability can be characterized [30–32].

In this paper, we wish to report a convenient and environmentally benign green route for the synthesis of novel high-performance PEIIs by using imidazolium-based ILs under one-step classical heating conditions. Therefore, a new aromatic and unsymmetrical diamine, 4,4'-(((2-(9-ethyl-carbazol-2-yl)-1H-imidazole-4,5-diyl)bis(4,1-phenylene))bis(oxy))bis(3-(trifluoromethyl)aniline), bearing polar CF_3 groups, ether linkage, bulky imidazole and carbazole rings was designed and successfully synthesized. This diamine was used for the synthesis of novel PEIIs in view of improving their solubility with outstanding thermal stability. These collective functional groups of highly polar CF_3 groups along with flexibility, unsymmetrical, and bulky pendant in the polymer backbone were expected to decrease the regularity of polymer chains, increasing the distance between the chains and weaken the intermolecular interaction of the chains. Therefore, as a result of higher barrier potential for free rotation, increasing interaction with polar solvent molecules and presence of chromophore would afford polymers with useful solubility, thermal and photophysical properties.

2. Results and discussion

2.1. Synthesis and characterization of diamine (4)

A new diamine, 4,4'-((4,4'-(2-(9-ethylcarbazol-2-yl)-1H-imidazole-4,5-diyl)bis(4,1 phenylene))bis(oxy))bis(3-(trifluoromethyl)aniline), was synthesized according to the synthetic route and

shown in **Scheme 1**. Condensation of 4,4'-dimethoxy benzyl with aqueous HBr and glacial acetic acid was applied for the synthesis of compound 1. The compound 2 was synthesized by nucleophilic aromatic substitution reaction of 4,4'-dihydroxy benzyl with 2-chloro-5-nitrobenzotrifluoride. The reaction between compound 2 and 9-ethyl-carbazole-2-carbaldehyde in ammonium acetate which is a well known synthetic method for preparation of imidazole ring was used to synthesize the compound 3. The catalytic hydrogenation of dinitro groups in compound 3 into the corresponding diamine was accomplished by using hydrazine hydrate in ethanol in the presence of a catalytic amount of Pd/C. The purity of all compounds was checked by thin-layer chromatography using ethylacetate/*n*-hexane mixture. The structure of diamine 4 was confirmed by elemental analysis, FT-IR, and ^1H and ^{13}C NMR spectroscopy. The FT-IR spectrum of compound 3 showed absorption bands at 1546 and 1349 cm^{-1} due to asymmetric and symmetric $-\text{NO}_2$ stretching vibrations. After reduction, absorption peaks related to NO_2 groups disappeared and new bands at 3478 and 3373 cm^{-1} due to N–H stretching were observed. The ^1H NMR spectrum of diamine 4 in **Fig. 1** and the assigned protons given in the experimental section has confirmed that the nitro groups were completely transformed into the amine groups by the high field shift of the aromatic protons and by the characteristic resonance of two different kind of protons: NH_2 protons at 5.47 and 5.52 ppm and N–H of imidazole ring at 12.5 ppm. The ^{13}C NMR spectrum of diamine 4 in **Fig. 2** showed 32 different carbon atoms for the aromatic segment and heterocyclic ring. The chemical shift in the upfield region (14.23 and 37.56 ppm) is ascribed to the resonance of aliphatic methyl group. Also, there are four quartet peaks because of the heteronuclear ^{13}C – ^{19}F coupling. The large quartet centered at about 123 ppm is due to the $-\text{CF}_3$ carbons. The one-bond C–F coupling constant in this case is about 270 Hz. The CF_3 -attached carbon also shows a clear quartet centered at about 122 ppm with a smaller coupling constant of about 32 Hz due to two-bond C–F coupling. These quartet signals corroborate the presence of CF_3 group in the synthesized compounds. Thus, all the spectroscopic data obtained by ^{13}C NMR and DEPT techniques were in good agreement with the expected chemical structures.

2.2. Polymers synthesis and characterization

Polycondensation in NMP/Py/ Ac_2O , is one of the effective methods for the synthesis of aromatic PIs. However, because of the usage of such aggressive solvents, partial hydrolysis of formed

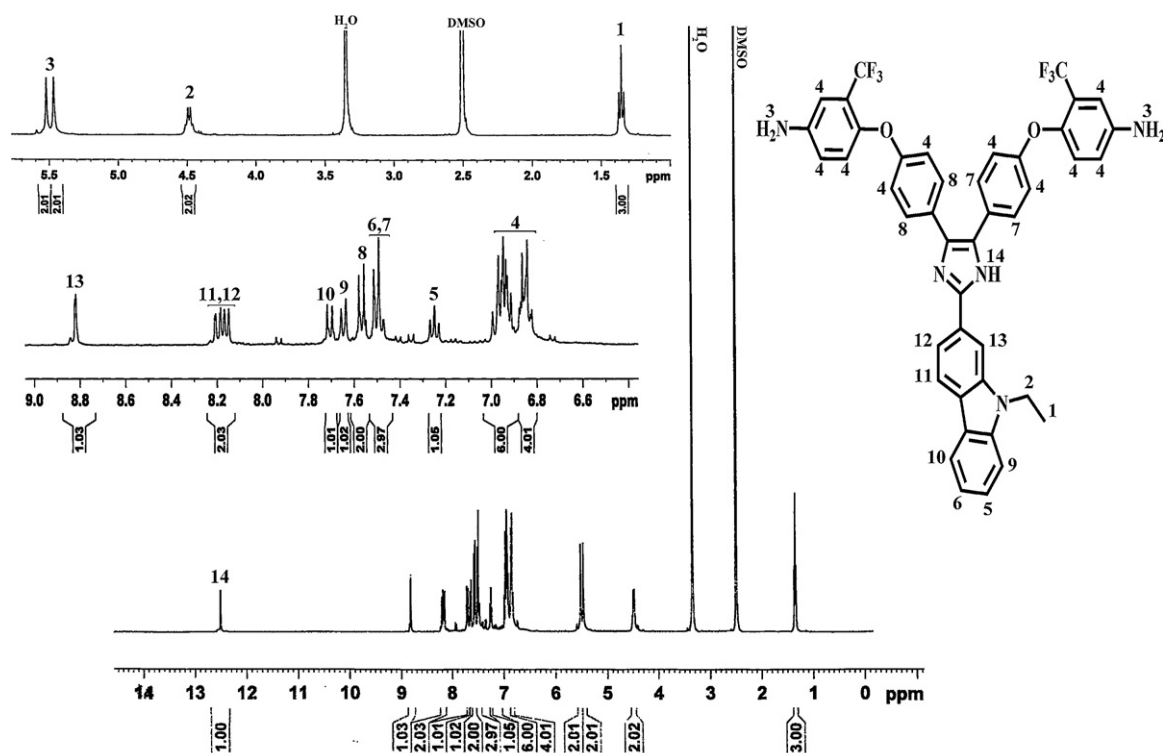


Fig. 1. ^1H NMR spectrum of diamine (4) in $\text{DMSO}-d_6$.

polymers during their isolation and purification complicates this process as well. For the advancement of ecological safety and improvement of technological ability of this process, IL solvents based on the imidazolium cations were used as a reaction medium. The reaction proceeded efficiently in ILs allowing PEII synthesis by direct polycondensation of dianhydride and diamines without using NMP, Ac_2O and pyridine (Py). Room temperature ILs, predominantly those based on substituted imidazolium cations which can be prepared simply from the commercially available starting materials, *N*-trimethylsilylimidazole and alkyl halides, were used in this investigation [10,33]. Thus, different symmetrical 1,3-dialkylimidazolium ILs bearing Br^- , PF_4^- and BF_6^- anions, shown in Table 1, were prepared and used as polycondensation agent. These ILs are soluble in the polar solvents such as water and methanol, which allowed the complete isolation of obtained

polymers. In order to find out the effect of ILs nature on the yield and viscosity of the polymer, the synthesis of PEII 1 was carried out in different imidazolium type ILs at a reaction temperature. IL needs to be liquid and thermally stable near the reaction temperature and a good solvent for initial monomers and the resulting polymers. These ILs were all very viscous liquids at room temperature. Therefore, the choice of polycondensation temperature (130°C) was being determined by the viscosity of the ILs and solubility of the diamine 4 and the corresponding polymers. Although PEII 1 was soluble in all used ILs, but as alkyl chain in IL increased the yield and viscosity of the polymer decreased. This may be due to the decrease of polarity of IL as a result of increase in the alkyl chain which explains the lower mobility of polymer chains in longer alkyl chain of ILs. The polymer PEII 1 with the highest yield and viscosity was obtained when [1,3-(Pr)₂im]Br was

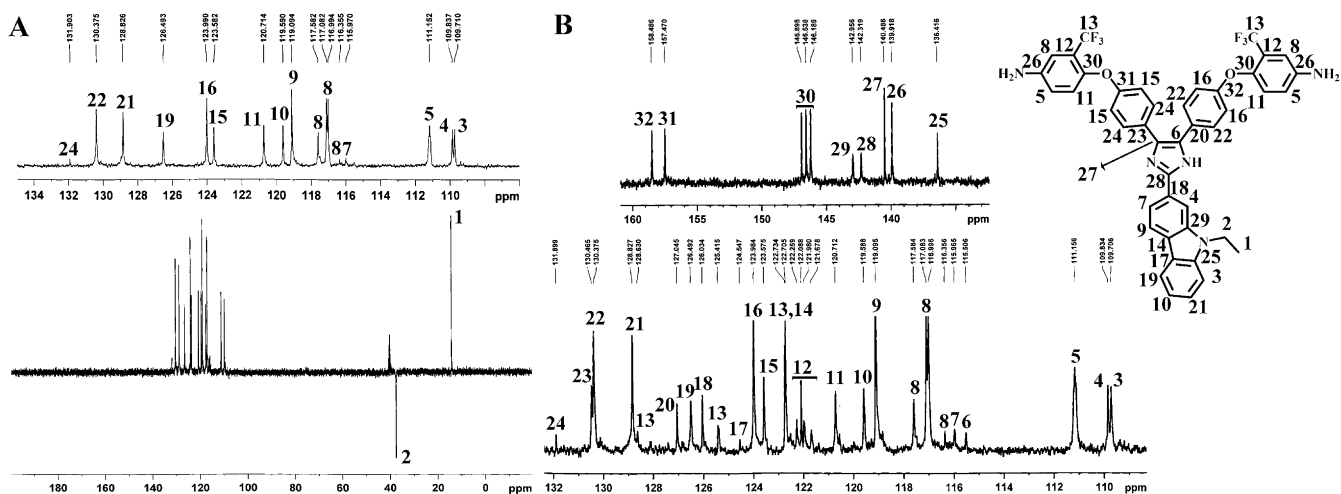
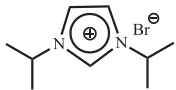

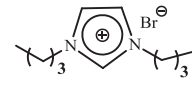




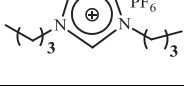


Fig. 2. ^{13}C NMR spectra of diamine (4) in $\text{DMSO}-d_6$: (A) DEPT and (B) normal.

Table 1
The influence of IL cation and anion upon yield and molecular weight (η_{inh}) of PEII 1.

Polymer	IL structure	IL	Yield (%)	η_{inh}^a
PEII 1		[1,3-Isopropyl ₂ im]Br	76	0.52
PEII 1		[1,3-Propyl ₂ im]Br	96	0.67
PEII 1		[1,3-Butyl ₂ im]Br	89	0.64
PEII 1		[1,3-Pentyl ₂ im]Br	83	0.55
PEII 1		[1,3-Hexyl ₂ im]Br	79	0.44
PEII 1		[1,3-Heptyl ₂ im]Br	81	0.43
PEII 1		[1,3-Butyl ₂ im]BF ₄	68	0.41
PEII 1		[1,3-Butyl ₂ im]PF ₆	64	0.33

^a Measured at a concentration of 0.5 g/dL in NMP at 25 °C.

used as the reaction media, as shown in Table 1, and this IL was also selected for the synthesis of other PEIIs. As far as anions were concerned, the best results were achieved in ILs with Br⁻. The optimum time of polycondensation was determined by measuring the yield and viscosity of PEII 1 in the selected IL and temperature, the results were shown in Fig. 3. Therefore all of the PEIIs (1–4) were prepared in two different reaction conditions; in direct polycondensation reactions by using NMP/Py/Ac₂O and by using only IL of [1,3-(Pr)₂im]Br. The results in Table 2 demonstrated the beneficial effect of using IL in the synthesis of PEIIs in addition to other useful properties such as non-volatility and reusability of ILs. Furthermore, removal of some chemicals (e.g. NMP, Py and Ac₂O)

which are essential in conventional direct polycondensation and also longer period of time (36 h vs. 10 h) increases the cost of polymerization as well as the environmental pollution which all together are the desired aspects for energy saving. The PEIIs were obtained as light brown powders with good yields, 81–96% after extraction with refluxing methanol for 24 h to remove low fraction oligomers, and their inherent viscosities were in the range of 0.37–0.67 dL g⁻¹ indicating medium molecular weights. The aforementioned results can serve as evidence that ILs are the effective alternative to the previously used aggressive and toxic media. Because of their nature the ILs have very low vapor pressure and are characterized by the absence of strong acid or alkaline

Table 2
Product yields and solubility of PEII 1–PEII 5.

Code	Solvent											
	Yield (%)	η_{inh} (dL/g) ^a	DMAc	DMF	NMP	DMSO	Py	DO	CHCl ₃	CH ₃ CN	<i>m</i> -cresol	
PEII 1	96	0.67	++	++	++	++	+	±	±	-	+	
PEII 2	94	0.51	++	++	++	++	++	±	+	-	++	
PEII 3	91	0.65	++	++	++	++	++	±	±	-	+	
PEII 4	81	0.37	++	++	++	++	++	+	++	±	++	
PEII 5	94	0.67	++	++	++	++	++	+	++	±	++	
PEII 1a	91	0.58	++	++	++	++	+	-	-	-	±	
PEII 2a	88	0.46	++	++	++	++	++	±	±	-	++	
PEII 3a	84	0.61	++	++	++	++	+	±	±	-	+	
PEII 4a	80	0.33	++	++	++	++	++	±	++	±	++	
PEII 5a	90	0.55	++	++	++	++	++	±	++	±	++	

++, soluble at room temperature; +, soluble on heating at 60 °C; ±, partially soluble on heating at 60 °C; -, insoluble on heating at 60 °C. PEII 1–PEII 5 and PEII 1a–PEII 5a were synthesized in IL and NMP/Ac₂O/Py media, respectively.

^a Measured at a polymer concentration of 0.5 g/dL in NMP at 30 °C.

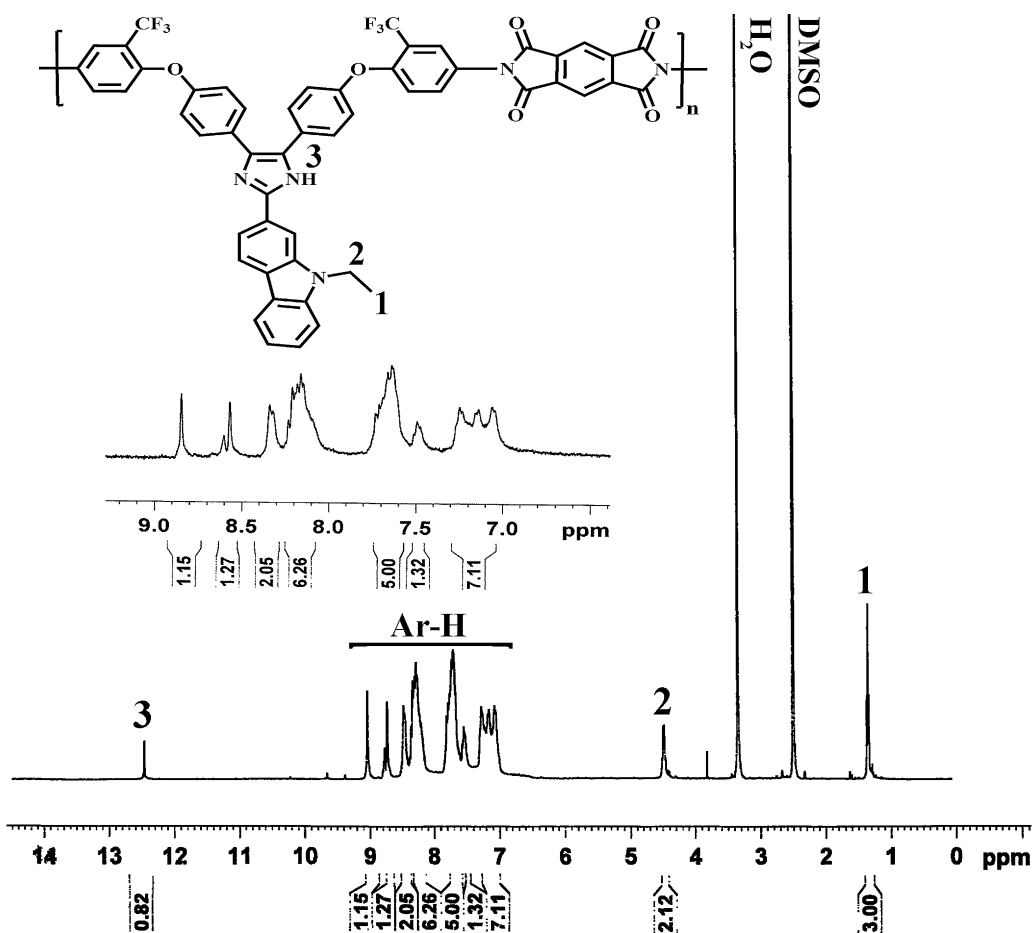


Fig. 3. Optimum conditions for the synthesis of PEII 1 in IL.

properties; therefore, the risk of polymer's hydrolysis at the isolation along with the necessity of its thorough purification are no longer relevant. The polymer structures were confirmed by elemental analysis, FT-IR and ^1H NMR spectroscopic techniques. The characteristic absorption bands of the five-membered imide ring appeared at 1785 and 1723 cm^{-1} , corresponding to asymmetric and symmetric $\text{C}=\text{O}$ stretching, at 1375 cm^{-1} related to $\text{C}-\text{N}$ stretching, and at 1094 and 763 cm^{-1} because of imide ring deformation. The ^1H NMR spectrum of PEII 1 in $\text{DMSO}-d_6$, Fig. 4, showed peaks of aromatic protons at 7.06 – 8.85 ppm and N–H imidazole proton at 12.61 ppm, all of which were well assigned to the supposed chemical structure and no peaks attributable to amic

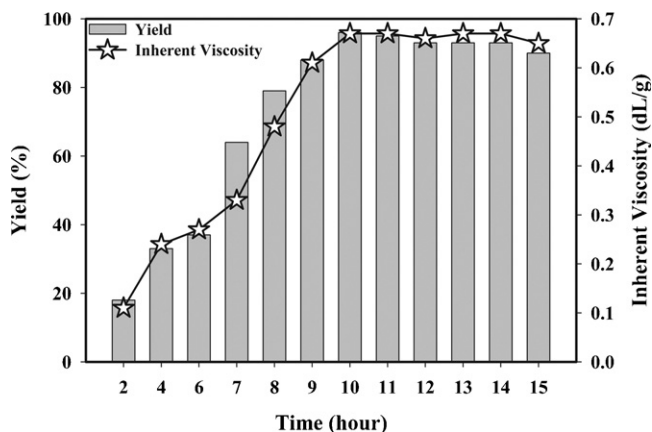


Fig. 4. ^1H NMR spectrum of PEII 1 in $\text{DMSO}-d_6$.

acids were detected. The integration ratio of these peaks also agreed with the structure. The elemental analysis values generally agreed with the calculated values for the proposed structures of polymers.

2.3. X-ray diffraction of the PEIIs

The crystallinity of the prepared PEIIs as powder samples was examined by WAXD analysis with graphite-monochromatized

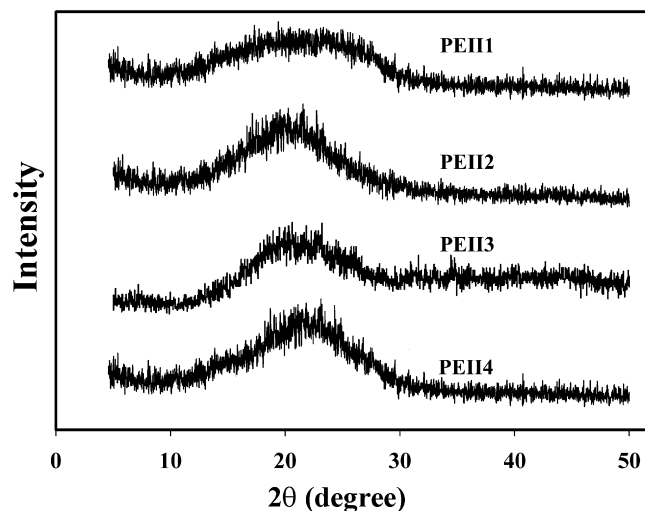


Fig. 5. X-ray diffraction patterns of PEIIs.

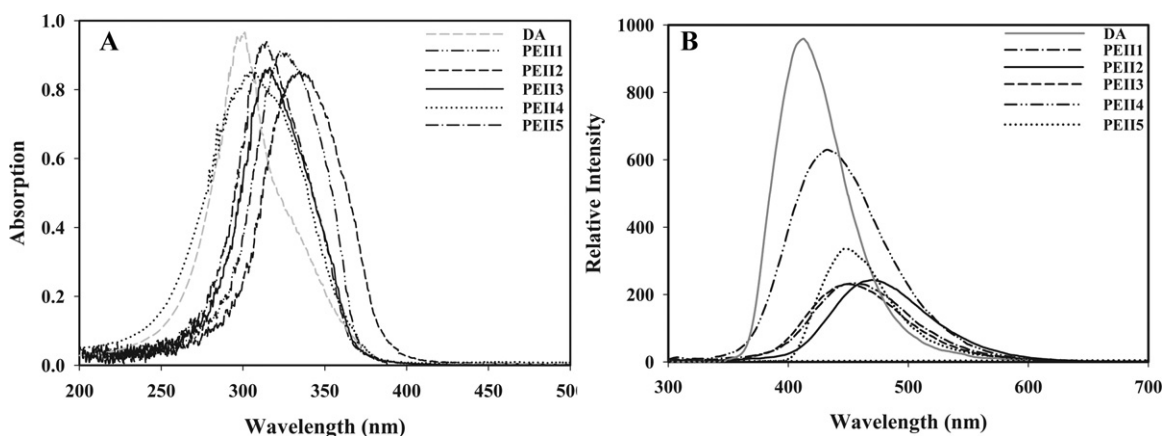


Fig. 6. UV-vis and fluorescence spectrum of diamine (4) and PEII 1–PEII 5.

Table 3

Optical properties data of PEII 1–PEII 5.

Polymer	λ_{abs} (nm) ^a	λ_{em} (nm) ^a	λ_{abs} (nm) ^a	λ_{em} (nm) ^a	Φ_f (%) ^b	Film thickness (μm)	λ_o (nm) ^c	Transparency (%) ^d
PEII 1	321	455	324	463	0.10	51	326	87
PEII 2	327	470	333	474	0.12	60	337	85
PEII 3	308	446	315	451	0.09	57	321	86
PEII 4	301	431	302	433	0.25	55	304	87
PEII 5	308	443	313	447	0.15	51	318	88

Polymer concentration of 0.20 g/dL in NMP.

^a UV-vis and fluorescence spectra of the PEIIs in solution (a) and film (b), respectively.

^b Fluorescence quantum yield relative to 10^{-5} M quinine sulfate in 1 N H_2SO_4 (aq) ($\Phi_f=0.55$) as a standard.

^c Cut-off wavelength.

^d Transparency at 400 nm.

Cu K α radiation and with 2θ ranging from 0 to 50° . The WAXD patterns of these polymers showed an amorphous nature and the results were shown in Fig. 5. The amorphous nature of the PEIIs can be attributed to their unsymmetrical structural units and the bulky CF_3 groups, which reduced the intra- and interpolymer chain interactions, resulting in loose polymer chain packaging and aggregates. Therefore, the amorphous nature of the resulting PEIIs would endow them a good solubility.

2.4. Solubility

The solubility of the resulting PEIIs was investigated in 5% (w/v) in different organic solvents, and the results were tabulated in Table 2. These polymers exhibited good solubility behavior in polar aprotic solvents such as NMP, *N,N*-dimethylacetamide (DMAC), *N,N*-dimethylformamide (DMF), dimethyl sulfoxide (DMSO), and even in less polar solvents like pyridine and *m*-cresol, but showed poorer solubility in dioxane (DO) and chloroform (CHCl_3) due to the low value of dielectric constant of these solvents. The good solubility of these PEIIs might be attributed to the unsymmetrical structure of the diamine, introduction of the flexible ether linkages and the bulky pendant of carbazole and CF_3 groups in the polymer backbone which decreased the interaction between polymer chains and loosen their packing efficiency, resulting in the increase of free volume in the polymers and easier diffusion of solvent molecules. On the other hand, the unsymmetrical structure could result in the random orientation in consecutive repeating units along the polymer main chain, which are naturally different in rigidity and degree of bending and lead to backbone randomization. This backbone randomization should also make a contribution to the high solubility of these polymers. In addition, the solubility varies depending upon the dianhydride used. PEIIs synthesized from aliphatic dianhydride (PEII 4) exhibited good solubility behavior in Py and *m*-cresol in comparison with the

other PEIIs. It should be noted that good solubility in low-boiling point solvents is critical for preparing objects at a relatively low processing temperature which is desirable for advanced micro-electronics manufacturing applications.

2.5. Photophysical properties

The UV-vis absorption and fluorescence spectra of diamine (2×10^{-5} M) and PEIIs (0.2 g/dL) in dilute NMP solution were shown in Fig. 6 and the extracted data were tabulated in Table 3. The diamine and PEIIs exhibited strong UV-vis absorption bands with maxima at 302 nm and in the range of 301–327 nm, respectively, assignable mainly to the π - π^* and also n - π^* transitions. A slightly red shift is observed in the spectra of PEIIs

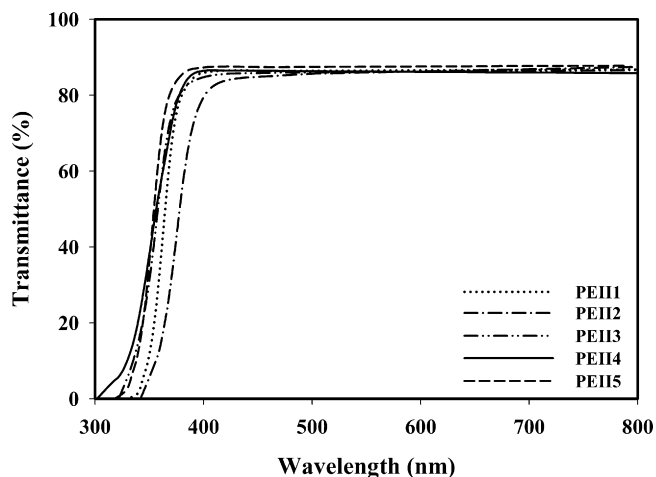


Fig. 7. Transmission UV-vis absorption spectra of PEII 1–PEII 5 films.

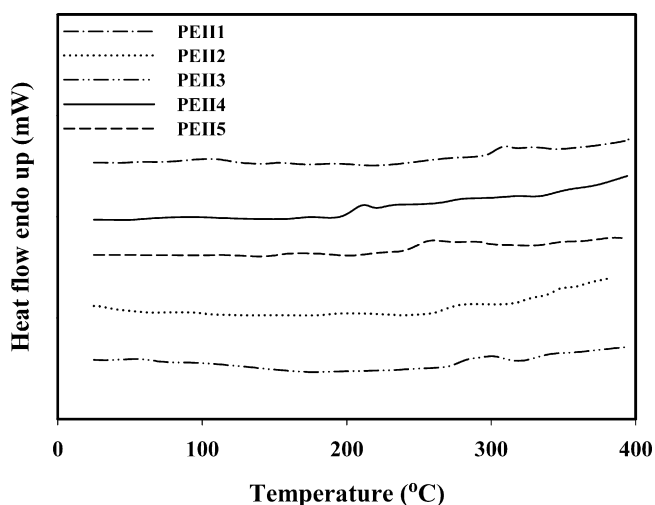


Fig. 8. DSC curves of PEII 1–PEII 5 under N₂ at 10 °C/min.

in comparison with the absorption spectrum of the diamine which can be due to expansion of conjugation system. Figs. 6a and 7 depict the UV–vis absorption and transmittance spectra of trifluoromethylated PEIIs films (50 μm thick), respectively, and the data were listed in Table 3. The cut-off wavelength (λ_0) values of the PEII films ranged from 302 nm to 333 nm, and the optical transmittance values at 400 nm are higher than 80%. These PEIIs with CF₃ pendants have smaller λ_0 values and higher optical transparency. These polymers also show color from pale yellow to colorless in nature. A possible explanation is that the bulky and strong electron-withdrawing CF₃ group in the diamine structure is presumably effective in decreasing the intermolecular and intramolecular charge–transfer complexes (CTC) between polymer chains as a result of steric hindrance and the inductive effect. The maximum emission ($\lambda_{\text{max(em)}}$) of the diamine in NMP solution (2×10^{-5} mol L⁻¹) was observed at 449 nm. The Fluorescence spectra of PEIIs in NMP solutions (0.2 g/dL) and in solid state exhibited high-intensity maximum around 470 nm for aromatic PEIIs (PEII 2) and 432 nm for the aliphatic PEII (PEII 4), respectively. To measure the fluorescence quantum yields (Φ_f), dilute polymer solutions (0.2 g/dL) in NMP were prepared. A 0.1 N solution of quinine in H₂SO₄ ($\Phi_f = 0.55$) was used as reference according to the literature [34]. The Φ_f values were 0.35 for the diamine, 0.25 for the aliphatic PEII and 0.09–0.12 for the aromatic PEIIs. The blue shift and higher fluorescence quantum yield of the aliphatic PEII 4 compared with the aromatic PEIIs could be attributed to reduced conjugation and capability of charge–transfer complex formation by the aliphatic dianhydride with the electron-donating diamine moiety in comparison to the stronger electron-accepting aromatic dianhydrides.

2.6. Thermal properties

DSC and TGA were applied to evaluate the thermal properties of the PEIIs. The DSC and TGA curves of the PEIIs are shown in Figs. 8 and 9, respectively, and thermal analysis data from the original curves were summarized in Table 4. The absence of melting peak in DSC thermograms and the results from X-ray patterns supported the generally amorphous nature of the PEIIs. The amorphous nature of these polymers can be attributed to their asymmetric structural unit and bulky pendent group which decreased the intra and inter-chain interactions, resulting in loose polymer chain packaging and aggregates. The T_g values of the PEIIs are in the range of 204–302 °C. As we expected, the T_g values depended on the structure of the dianhydride component and decreased with

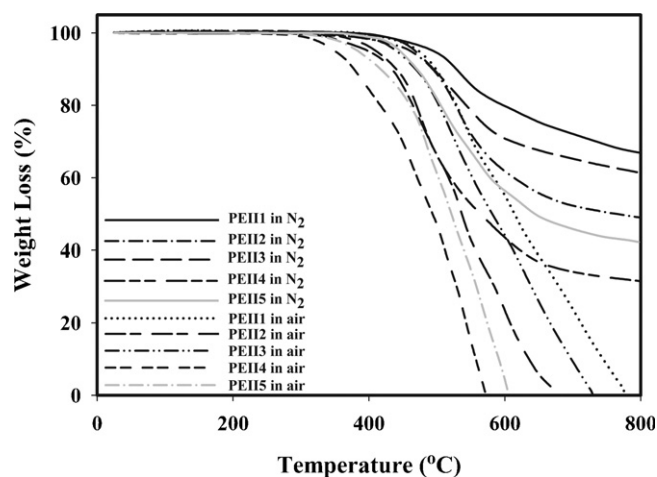


Fig. 9. TGA curves of PEII 1–PEII 5 under N₂ and air at 10 °C/min.

increasing flexibility of the polymers backbone. PEII 4, obtained from bicyclo[2.2.2]oct-7-ene-2,3,5,6-tetracarboxylic dianhydride, showed the lowest T_g because of the presence of flexible ether linkage between the phthalimide units. PEII 1, derived from pyromellitic dianhydride, exhibited the highest T_g because of having rigid polymer backbone. The T_g values of these polymers are lower than analogous PEIIs (T_g , 240–306 °C, which suggests that the nonlinear structure in the polymer backbone decreased the intermolecular interactions in these polymers, thus led to lower T_g values [35]. Thermal stability of PEIIs was evaluated by TGA in N₂ and air atmosphere at a heating rate 10 °C/min and the curves are shown in Fig. 9. The $T_{10\%}$ values of the PEIIs were in the range 441–528 and 382–494 °C in N₂ and air, respectively, and the amount of residue at 800 °C in N₂ was up to 60%. As can be seen in Table 4, thermal stability of these polymers based on the $T_{10\%}$ values and the amount of remained char at 800 °C is higher in N₂ atmosphere than those obtained in air. This difference can be due to thermal oxidation of the polymer sample at high temperature in air which resulted in thermal breakdown of polymer chains. It is concluded from Table 4 data that PEIIs with the aliphatic unit in the backbone such as PEII 4 and PEII 5 (or PEII 4a and PEII 5a) exhibited higher difference in thermal stability, or lower thermal stability, when comparing $T_{10\%}$ in air and in N₂. Comparing the $T_{10\%}$ of polymers in Table 4, it is observed that introduction of aliphatic trifluoromethyl decrease thermal stability of polymer at high temperatures in N₂ or in air. According to the results reported by other researchers [19],

Table 4
Thermal properties of PEII 1–PEII 5.

Polymer	T_g (°C) ^a	$T_{10\%}$ (°C) ^b	$T_{10\%}$ (°C) ^c	Char yield ^d	LOI (%) ^e
PEII 1	302	528	494	67	44
PEII 2	272	495	435	50	37
PEII 3	290	499	472	61	42
PEII 4	204	441	382	32	30
PEII 5	253	472	415	43	35
PEII 1a	294	511	486	61	42
PEII 2a	269	469	418	41	34
PEII 3a	288	477	459	52	38
PEII 4a	204	440	382	32	30
PEII 5a	250	463	402	39	33

PEII 1–PEII 5 and PEII 1a–PEII 5a were synthesized in IL and NMP/Py/Ac₂O media, respectively.

^a T_g was recorded in DSC at 10 °C/min in N₂.

^b Temperature at which 10% weight loss was recorded by TGA in N₂.

^c Temperature at which 10% weight loss was recorded by TGA in air.

^d Percentage weight of char remained of TGA analysis at 800 °C in N₂.

^e Limiting oxygen index percent evaluating at char yield 800 °C.

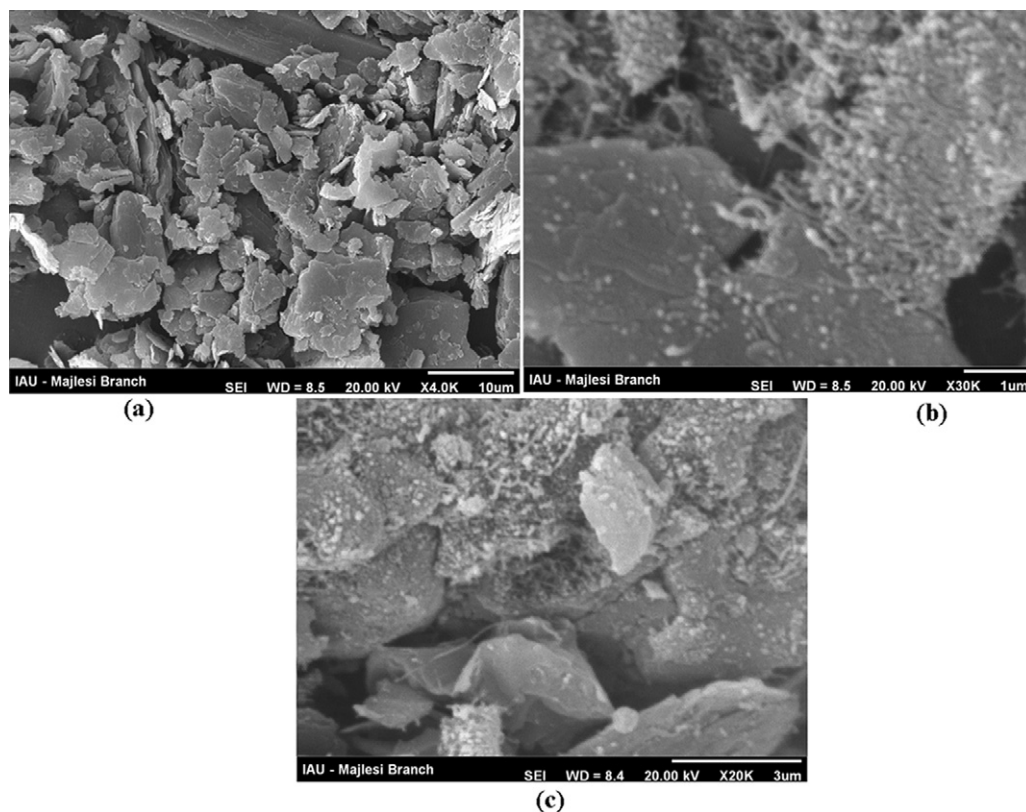


Fig. 10. SEM image of a graphite layer (a), graphite layer with MWCNTs (b) and PEII 1-modified carbon nanotubes paste electrode (c).

polyimides containing trifluoromethyl showed higher or comparable thermal stability than non-fluorinated polyimides. Char yield can be used as criteria for evaluating limiting oxygen index (LOI) of the polymers in accordance with Van Krevelen and Hoftyzer equation [36]. $LOI = 17.5 + 0.4 CR$ where CR = char yield. The char yield determines the flame retardency of a polymer. If it has a higher retardency, then it has greater tendency to self-extinguish a flame. The T_{10} values in N_2 and air and the LOI values calculated based on their char yields at 800 °C were given in Table 4. The data from thermal analysis indicated that the resulting polymers exhibited fairly high thermal stability. This explains that introduction of strong electron negativity of $-CF_3$ groups might have enhanced the polarity of the polymer, which should restrict the

movement of polymer-link and led to better thermal stability [37,38].

2.7. SEM characterization

Fig. 10 shows typical SEM images of carbon paste electrode (CPE), multiwall carbon nanotubes paste electrode (MWCNTPE) and MWCNTPE modified with PEIIs. It can be seen that on the surface of CPE (Fig. 10a), the layer of irregular and isolated flakes of graphite powder was present. After MWCNTs added to the carbon paste matrix, it can be seen in Fig. 10b that MWCNTs were distributed on the electrode with special three-dimensional structure, indicating that the MWCNTs were successfully modified

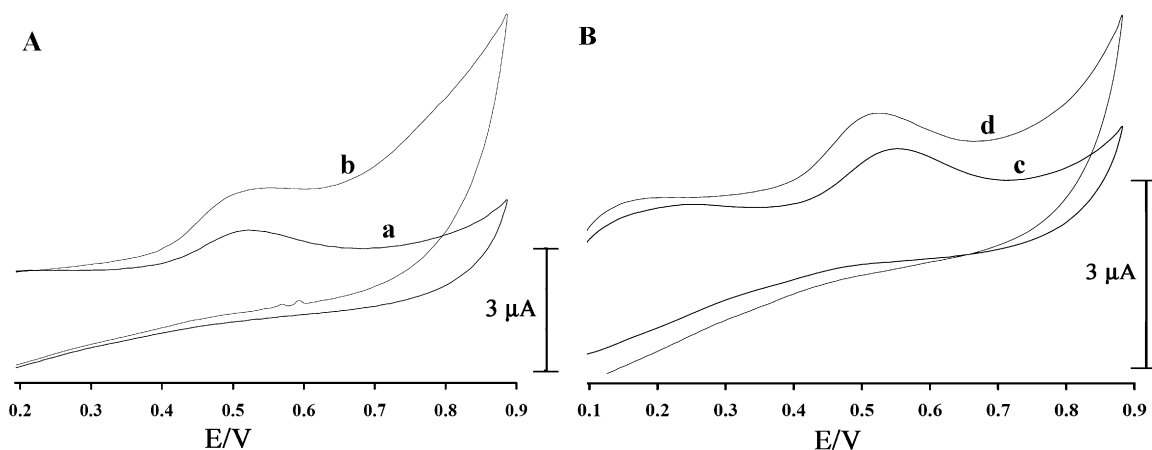


Fig. 11. Cyclic voltammograms of the monomer, PEII 1 with modified CPE (a and b), cyclic voltammograms of the PEII 2 without and with modified CPE (c and d) at a scan rate of 100 mV/s.

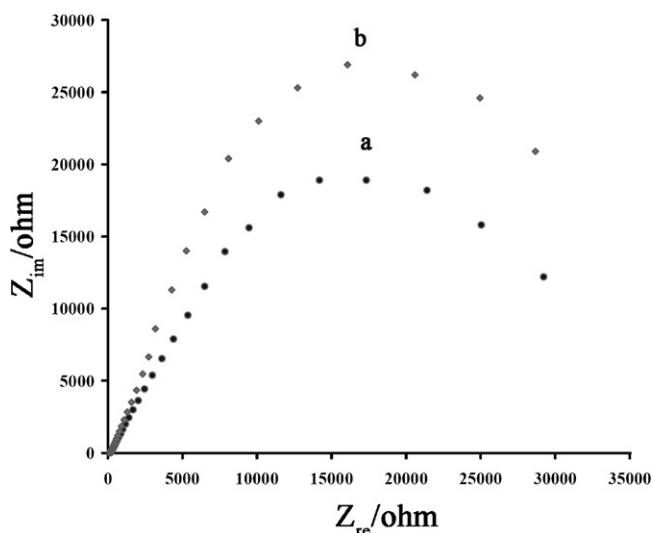


Fig. 12. Nyquist diagrams of the multiwall carbon nanotubes paste electrode modified with monomer (a) and PEII 1 (b) in PBS (pH 7.0).

on the MWCNTPE. Also, it can be clearly seen in Fig. 10c that the polymer has been dispersed in modified electrode.

2.8. Electrochemical investigation

The main object of this investigation was to study the electrochemical behavior of these PEIIs. Imidazol group can be oxidized at a suitable potential in electrochemical process [39]. Fig. 11A(a) shows cyclic voltammogram of multiwall carbon paste electrode modified with the diamine. An oxidation peak at potential ≈ 700 mV can be seen with low current which is related to the imidazol ring in the diamine structure. Fig. 11A(b) shows cyclic voltammogram of the polymer (PEII 1) paste with carbon used as electrode. As can be seen in this figure, there is a large oxidation current which can be attributed to the oxidation of imidazole rings in the polymer chains. The effect of MWCNTs on the oxidation peak current and peak potential was studied and the cyclic voltammograms for the polymer-carbon paste electrode were compared, in Fig. 11B, with the voltammogram of the electrode paste with MWCNT. As can be seen in these figures, addition of MWCNTs into the polymer carbon paste matrix increases the oxidation peak current and decreases the potential. This phenomenon is related to the unique electrochemical properties of CNTs with polymer and carbon paste as electrode [40,41]. MWCNTs will definitely improve the characteristics of electrochemical oxidation of polymer. Electrochemical impedance spectroscopy (EIS) was also employed to investigate the oxidation of the diamine and PEIIs at the surface of carbon nanotubes paste electrode. Fig. 12(a) and (b) compares the Nyquist diagram of the multiwall carbon nanotubes paste electrode modified with diamine and PEII 1 in phosphate buffer solution (PBS) (pH = 7.0), respectively. Under these conditions, charge transfer resistance (R_{ct}) is the only element that has a simple physical meaning describing how fast the rate of charge transfer is during the oxidation of imidazol groups. It is known that the amount of R_{ct} has reverse relationship with electrochemical activity of the species. In fact, with increasing electrochemical oxidation peak current, the value of R_{ct} decreased [41]. The R_{ct} values for the diamine and PEIIs were found 110 K Ω and 95 K Ω (Fig. 12 curves (a) and (b)), respectively. It is interesting to note that the result obtained with EIS is very similar to those obtained from cyclic voltammetry.

3. Conclusions

A novel trifluoromethyl-substituted diamine bearing imidazole and carbazole rings with an asymmetric molecular structure, 4,4'-(4,4'-(2-(9-ethyl-carbazol-2-yl)-1H-imidazole-4,5-diyl)bis(4,1-phenylene))bis(oxy) bis(3-(trifluoromethyl)aniline), has been successfully synthesized from readily available reagents. The diamine was polymerized with several aromatic and aliphatic dianhydrides via a conventional two-stage method including poly(amic acid) formation and chemical imidization in NMP solvent and a single-stage method in IL without using chemical imidization agents. In general, the results demonstrated the beneficial effects of using IL media in the synthesis of these PEIIs, such as good yields and moderate viscosity, shorter period of reaction time, not being needed to remove some chemicals (e.g. NMP, Py and Ac₂O), non-volatility and reusability, as well as the environmental pollution. Because of the presence of polar CF₃ and aryl ether groups along the polymer backbone together with the asymmetric structure of the repeating unit, these amorphous polymers exhibited excellent solubility in many organic solvents and could be solution cast into transparent tough films. They also showed high thermal stability with high optical transparency. Therefore, these PEIIs may be considered as promising processable high temperature materials for applications in microelectronic and optical devices.

4. Experimental

4.1. Materials

All starting materials and reagents were purchased from either Merck or Fluka (Germany) through a local agency. *N*-methyl-2-pyrrolidinone (NMP) and pyridine (Py) were purified by distillation under reduced pressure over calcium hydride and stored over 4 Å molecular sieves. Dianhydrides such as 3,3',4,4'-benzophenone tetracarboxylic dianhydride, pyromellitic dianhydride, 4,4'-oxydiphthalic anhydride and bicyclo[2.2.2]oct-7-ene-2, 3, 5, 6-tetracarboxylic dianhydride were dried in a vacuum oven at 110 °C for 5 h. Phosphate buffer (sodium dihydrogen phosphate and disodium monohydrogen phosphate plus sodium hydroxide, 0.1 mol L⁻¹) solution with pH = 7.0 value was used. Spectrally graphite powder (particle size <50 μ m), multiwall carbon nanotubes (>90%, MWCNTs, $d \times l = (70\text{--}90 \text{ nm}) \times (5\text{--}9 \mu\text{m})$), and high viscosity paraffin ($d = 0.88 \text{ kg/L}$) were purchased (Fluka) and used for preparation of carbon paste electrodes.

4.2. Measurements

Proton and carbon nuclear magnetic resonance (¹H NMR and ¹³C NMR) spectra were recorded on a 400 MHz Bruker (Ettlingen, Germany) instrument using DMSO-*d*₆ as solvent and tetramethyl silane as an internal standard. Elemental analyses performed by a CHN-600 Leco elemental analyzer. Melting point (uncorrected) was measured with a Barnstead Electrothermal engineering LTD 9200 apparatus. Inherent viscosities (at a concentration of 0.5 g/dL) were measured with an Ubbelohde suspended-level viscometer at 25 °C using NMP as solvent. Qualitative solubility was determined using 0.05 g of the polymer in 0.5 mL of solvent. Thermogravimetric analysis (TGA) was performed with the DuPont Instruments (TGA 951) analyzer well equipped with a PC at a heating rate of 10 °C/min under N₂ and air atmosphere (5, 10, 15 and 20 °C/min) and in the temperature range of 25–650 °C. Differential scanning calorimeter (DSC) was recorded on a Perkin Elmer pyris 6 DSC under nitrogen atmosphere at a heating rate of 10 °C/min. Glass-transition temperatures (T_g) values were read at the middle of the transition in heat capacity and were taken from the second heating scan after cooling from 350 °C at a cooling rate

of 10 °C/min. Ultraviolet–visible and fluorescence emission spectra were recorded on a Cecil 5503 (Cecil Instruments, Cambridge, UK) and Perkin-Elmer LS-3B spectrophotometers (Norwalk, CT, USA) (slit width = 2 nm), respectively, using a dilute polymer solution (0.20 g/dL) in DMSO. X-ray powder diffraction patterns were recorded by an X-ray diffractometer (GBC MMA instrument) with Be-filtered Cu K (1.5418 Å) operating at 35.4 kV and 28 mA. The 2θ scanning range was set between 4° and 50° at a scan rate of 0.05°/s. Cyclic voltammetry (CV) was performed in an analytical system, micro-Autolab, potentiostat/galvanostat connected to a three-electrode cell, Metrohm Model 663 VA stand, linked with a computer (Pentium IV, 2.67 GHz) and with micro-Autolab software. The prepared electrodes with CNTs and polymers were characterized by scanning electron microscopy (SEM; Seron Tech. AIS 2100). All the voltammetric measurements were performed using an Autolab PGSTAT 302N, potentiostat/galvanostat (Utrecht, The Netherlands) connected to a three-electrode cell, Metrohm (Herisau, Switzerland) Model 663 VA stand, linked with a computer (Pentium IV, 1200 MHz) and with Autolab software. A platinum wire was used as the auxiliary electrode. Modified multiwall carbon nanotubes paste electrode (MWCNTPE) and Ag/AgCl/KCl_{sat} were used as the working and reference electrodes, respectively. For impedance measurements, a frequency range of 100 kHz to 0.1 Hz was employed. The AC voltage amplitude used was 5 mV, and the equilibrium time was 10 min. The electrode prepared with carbon nanotubes was characterized by scanning electron microscopy (SEM) (Seron Tech. AIS 2100). A digital pH/mV-meter (Metrohm model 710) was applied for pH measurements.

4.3. Ionic liquids synthesis

All room temperature ILs were prepared according to the procedures reported in the literatures [10,33]. The structure of the prepared ILs was given in Table 1, and they were all very viscous liquids at room temperature.

4.4. Monomer synthesis

The following synthetic steps were used to synthesis the target diamine, as outlined in Scheme 1.

4.4.1. Synthesis of 4,4'-dihydroxy benzyl (1)

Into a 100 mL round-bottomed two-necked flask equipped with a magnetic stirrer bar and a reflux condenser, 4,4'-dimethoxybenzil (2 g, 0.0075 mmol), aqueous HBr (15 mL, 48%) and glacial acetic acid (15 mL) were placed. The reaction mixture was refluxed for 24 h, after cooling to room temperature, was poured into 100 mL water. Ethyl acetate was added to the mixture to give two phases of which the organic phase containing the product was separated and dried over magnesium sulfate for 12 h. The solvent was removed under reduced pressure and the obtained yellow precipitate was washed thoroughly with water and then dried in a vacuum oven at 80 °C. Yield: 94% (1.7 g) and m.p.: 229–231 °C. FT-IR (KBr) at cm^{-1} : 3400 (OH phenol), 3045 (C–H aromatic), 1646 (C=O), 1576 (C=C), 1223 (C–O). ¹H NMR (400 MHz, DMSO-*d*₆): δ 6.91–6.95 (d, 4H, *J* = 8.0 Hz), 7.73–7.77 (d, 4H, *J* = 8.0 Hz), 10.84 (s, 2H).

4.4.2. Synthesis of 1, 2-bis(4-(4-nitro-2-(trifluoromethyl)phenoxy)phenyl)ethane-1,2-dione (2)

Into a 100 mL round-bottomed two-necked flask equipped with a magnetic stirrer bar and a reflux condenser, 4,4'-dihydroxy benzil (1.21 g, 0.005 mol) and 1-chloro-4-nitro-2-(trifluoromethyl)benzene (2.25 g, 0.01 mol) were dissolved in 10 mL DMAc, and potassium carbonate (1.38 g, 0.01 mol) was added to the

solution. After 30 min of stirring at room temperature, the mixture was heated at 110 °C for 6 h and then was poured in 100 mL distilled water. The yellow precipitate was filtered off and dried in a vacuum oven at 80 °C. Yield: 93% (2.9 g) and m. p: 157–160 °C.

FT-IR (KBr) at cm^{-1} : 3045 (aromatic C–H); 1621 (C=O); 1482 (C=C); 1534, 1353 (NO₂); 1268 (C–O) stretching. ¹H NMR (400 MHz, DMSO-*d*₆): δ 7.41 (d, 4H, Ar-H, *J* = 8.0 Hz), 7.46 (d, 2H, Ar-H, *J* = 8.0 Hz), 8.08 (d, 4H, Ar-H, *J* = 8.0 Hz), 8.54 (dd, 2H, Ar-H, *J* = 8.0 Hz), 8.57 (d, 2H, Ar-H, *J* = 2.8 Hz).

4.4.3. 2-(4,5-bis(4-(4-nitro-2-(trifluoromethyl)phenoxy)phenyl)-1H-imidazol-2-yl)-9-ethyl carbazole (3)

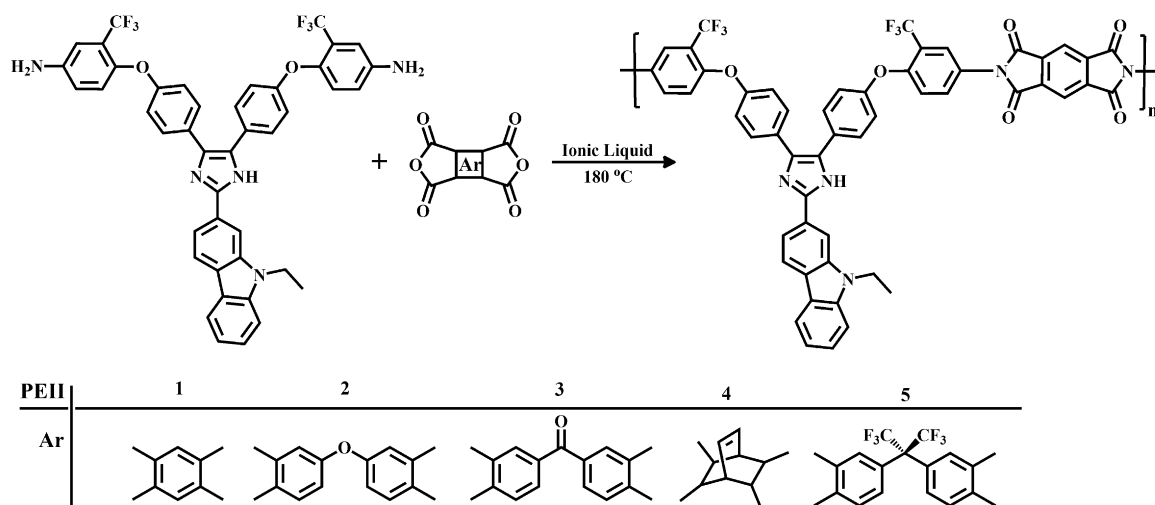
Into a 100 mL round-bottomed two-necked flask equipped with a condenser, a magnetic stirring bar and a nitrogen gas inlet tube, a mixture of 9-ethyl-carbazole-2-carbaldehyde (1.11 g, 0.005 mol), compound 2 (3.1 g, 0.005 mol), ammonium acetate (2.7 g, 0.035 mol), and glacial acetic acid (25 mL) was refluxed for 14 h. Upon cooling, the yellow precipitate was collected by filtration and washed with a mixture of ethanol/water (50/50, v/v) and dried in a vacuum oven at 80 °C. Yield: 91% (3.75 g) and m. p.: 170–173 °C.

FT-IR (KBr) at cm^{-1} : 3473 (NH, imidazole ring); 3062 (aromatic C–H); 2904 (aliphatic C–H); 1612 (C=N); 1586 (C=C), 1546, 1349 (NO₂); 1278 (C–N), 1237 (C–O–C). ¹H NMR (400 MHz, DMSO-*d*₆): δ 1.36 (t, 3H, CH₃), 4.50 (q, 2H, CH₂), 7.19 (d, 2H, Ar-H, *J* = 8.0 Hz), 7.23 (d, 2H, Ar-H, *J* = 8.0 Hz), 7.27 (t, 1H, Ar-H, *J* = 8.0 Hz), 7.36 (d, 2H, Ar-H, *J* = 8.0 Hz), 7.50 (t, 1H, Ar-H, *J* = 8.0 Hz), 7.66 (d, 2H, Ar-H, *J* = 8.0 Hz), 7.73 (d, 2H, Ar-H, *J* = 8.0 Hz), 7.77 (d, 2H, Ar-H, *J* = 8.0 Hz), 8.19 (d, 1H, Ar-H, *J* = 8.0 Hz), 8.24 (dd, 1H, Ar-H, *J* = 8.0 Hz), 8.48 (d, 2H, Ar-H, *J* = 2.8 Hz), 8.55 (dd, 2H, Ar-H, *J* = 8.0 Hz), 8.87 (d, 1H, Ar-H, *J* = 1.6 Hz), 12.57 (s, 1H, N–H imidazole ring). Anal. Calcd. for C₄₃H₂₇N₅O₆F₆ (823 g/mol): C, 62.69%; H, 3.28%; N, 8.50%. Found: C, 62.66%; H, 3.30%; N, 8.50%.

4.4.4. 4,4'-(4,4'-(2-(9-ethylcarbazol-2-yl)-1H-imidazole-4,5-diyl)bis(4,1-phenylene)) bis(oxy)bis(3-(trifluoromethyl) aniline) (4)

Into a 100 mL round-bottomed two-necked flask equipped with a magnetic stirring bar, a mixture of compound 3 (4.10 g, 0.005 mol) and Pd/C (0.1 g, 10%) were dispersed in 50 mL ethanol. The suspension was heated to reflux, and then 6 mL hydrazine monohydrate was added slowly to the mixture. After a further 8 h of reflux, the solution was filtered hot to remove Pd/C, and the filtrate was cooled to precipitate white crystals. The product was collected by filtration and dried in a vacuum oven at 80 °C. Yield: 86% (3.26 g) and m.p.: 155–157 °C.

FT-IR (KBr) at cm^{-1} : 3478, 3373 (NH₂), 3462 (N–H imidazole ring), 3051 (C–H aromatic), 2912 (aliphatic C–H); 1628 (C=N), 1597 (C=C), 1286 (C–N) and 1214 (C–O–C). ¹H NMR (400 MHz, DMSO-*d*₆): δ 1.35 (t, 3H, CH₃), 4.47 (q, 2H, CH₂), 5.47 (s, 2H, NH₂), 5.52 (s, 2H, NH₂), 6.82–6.99 (m, 10H, Ar-H), 7.25 (t, 1H, Ar-H), 7.47 (t, 1H, Ar-H), 7.49 (d, 2H, Ar-H, *J* = 8.0 Hz), 7.56 (d, 2H, Ar-H, *J* = 8.0 Hz), 7.64 (d, 1H, Ar-H, *J* = 8.0 Hz), 7.70 (d, 1H, Ar-H, *J* = 8.0 Hz), 8.15 (d, 1H, Ar-H, *J* = 8.0 Hz), 8.21 (dd, 1H, Ar-H, *J* = 8.4 Hz), 8.82 (d, 1H, Ar-H, *J* = 1.6 Hz), 12.51 (s, 1H, N–H imidazole ring). ¹³C NMR (400 MHz, DMSO-*d*₆, δ): 1 (14.23), 2 (37.56), 3 (109.71), 4 (109.83), 5 (111.16), 6 (115.51), 7 (115.97), 8 (116.36, 117.00, 117.08 and 117.58), 9 (119.09), 10 (119.59), 11 (120.71), 12 (121.68, 121.98, 122.09 and 122.26), 13 (122.70, 125.41, 125.42 and 128.63), 14 (122.73), 15 (123.57), 16 (123.98), 17 (124.55), 18 (126.03), 19 (126.49), 20 (127.04), 21 (128.83), 22 (130.37), 23 (130.46), 24 (131.90), 25 (136.42), 26 (139.92), 27 (140.49), 28 (142.32), 29 (142.96), 30 (146.19, 146.54 and 146.90), 31 (157.47), 32 (158.49). DEPT Technique (400 MHz, DMSO-*d*₆, δ): 1 (14.22), 2 (37.56), 3 (109.71), 4 (109.84), 5 (111.15), 7 (115.97), 8 (116.35, 116.99, 117.08 and 117.58), 9 (119.09), 10 (119.59), 11 (120.71), 15 (123.58), 16 (123.99), 19 (126.49), 21 (128.83), 22 (130.37), 24



Scheme 2. Polycondensation reactions of the diamine with different dianhydrides.

(131.90). Anal. Calcd. for $C_{43}H_{31}N_5O_2F_6$ (763 g/mol): C, 67.62%; H, 4.06%; N, 9.17%. Found: C, 67.59%; H, 4.10%; N, 9.16%.

4.5. Polymer synthesis

4.5.1. Method I: direct polycondensation using NMP/Py/ Ac_2O

The following general procedure was used for the preparation of all PEIIs. A 100 mL three-necked round-bottomed flask equipped with a condenser, a magnetic stirrer bar, a nitrogen gas inlet tube and a calcium chloride drying tube was charged with 1 mmol (0.51 g) diamine and 10 mL dry NMP and the mixture was stirred at room temperature for 0.5 h. Thereafter, 1 mmol of a dried dianhydride was added and the mixture was stirred at room temperature for 24 h, forming a viscous solution of poly(amic acid) (PAA) in NMP. The chemical imidization of PAA was carried out by adding 3 mL of a mixture of acetic anhydride/pyridine (6/4, v/v) into the solution while stirring at room temperature for 1 h. The mixture was then stirred at 130 °C for 12 h to yield a homogeneous polymer solution, which was poured slowly into methanol to yield a precipitate that was collected by filtration, washed thoroughly with hot methanol and dried at 80 °C in a vacuum oven overnight. The yields were in the range of 80–91%.

4.5.2. Method II: direct polycondensation using ILs

The following general procedure, as illustrated in Scheme 2, was used for the preparation of PEIIs from the diamine and various aliphatic and aromatic dianhydrides.

In a 50 mL round-bottomed three-necked flask equipped with a dropping funnel, a reflux condenser and a magnetic stirrer bar, 1 mmol (0.51 g) diamine, 1 mmol tetracarboxylic acid dianhydride and 3 g of IL were stirred at room temperature for 10 min. The temperature was gradually elevated to 180 °C under an inert gas atmosphere and reaction mixture was held at such temperature and stirring for 10 h. An additional 0.5 g IL was added to the mixture. As the reaction proceeded, the solution became viscous. The reaction mixture was then cooled to room temperature and the resulting polymers were precipitated in 100 mL methanol. The precipitate was filtered and washed with hot water, and then was further purified by washing with refluxing methanol for 24 h in a Soxhlet apparatus to remove the low molecular weight oligomers. The inherent viscosity (η_{inh}) of the resulting PEIIs was between 0.37–0.67 dL g⁻¹, measured at a concentration of 0.5 g/dL in NMP at 25 °C. The above procedure was used for the preparation of all PEIIs given below.

4.5.2.1. PEII 1. 96% yield, FT-IR (KBr, cm⁻¹): 3435 (NH imidazole), 3072 (C–H aromatic), 1781, 1722 (C=O imide), 1608 (C=N imidazole), 1475 (C=C), 1370 (C–N) and 1250 (C–O). ¹H NMR (DMSO-*d*₆): δ 1.36 (t, 3H, CH₃), 4.48 (q, 2H, CH₂), 7.06–8.84 (m, 23H, Ar-H), 12.61 (s, 1H, N–H imidazole ring). Anal. Calcd. (%) for $(C_{53}H_{29}F_6N_5O_6)_n$: C, 67.30; H, 3.07; N, 7.41. Found: C, 67.22; H, 3.15; N, 7.39.

4.5.2.2. PEII 2. 94% yield, FT-IR (KBr, cm⁻¹): 3447 (NH imidazole), 3052 (C–H aromatic), 1782, 1725 (C=O imide), 1605 (C=N imidazole), 1483 (C=C), 1372 (C–N) and 1239 (C–O). ¹H NMR (DMSO-*d*₆): δ 1.42 (t, 3H, CH₃), 4.51 (q, 2H, CH₂), 7.26–8.93 (m, 27H, Ar-H), 12.75 (s, 1H, N–H imidazole ring). Anal. Calcd. (%) for $(C_{60}H_{33}F_6N_5O_7)_n$: C, 68.64; H, 3.15; N, 6.67. Found: C, 68.60; H, 3.19; N, 6.66.

4.5.2.3. PEII 3. 91% yield, FT-IR (KBr, cm⁻¹): 3448 (NH imidazole), 3056 (C–H aromatic), 1784, 1725 (C=O imide), 1603 (C=N imidazole), 1498 (C=C), 1370 (C–N) and 1248 (C–O). ¹H NMR (DMSO-*d*₆): δ 1.31 (t, 3H, CH₃), 4.44 (q, 2H, CH₂), 7.07–8.57 (m, 27H, Ar-H), 12.58 (s, 1H, N–H imidazole ring). Anal. Calcd. (%) for $(C_{59}H_{33}F_6N_5O_7)_n$: C, 68.27; H, 3.18; N, 6.75. Found: C, 68.26; H, 3.19; N, 6.73.

4.5.2.4. PEII 4. 81% yield, FT-IR (KBr, cm⁻¹): 3447 (NH imidazole), 3056 (C–H aromatic), 2957 (C–H aliphatic), 1786, 1721 (C=O imide), 1605 (C=N imidazole), 1497 (C=C), 1369 (C–N) and 1261 (C–O). ¹H NMR (DMSO-*d*₆): δ 1.36 (t, 3H, CH₃), 2.34 (m, 2H, CH₂), 2.66 (m, 4H, CH), 4.48 (q, 2H, CH), 6.71 (m, 2H, C=CH), 7.02–8.68 (m, 21H, Ar-H), 12.56 (s, 1H, N–H imidazole ring). Anal. Calcd. (%) for $(C_{55}H_{35}F_6N_5O_6)_n$: C, 67.69; H, 3.59; N, 7.18. Found: C, 67.66; H, 3.61; N, 7.18.

4.5.2.5. PEII 5. 94% yield, FT-IR (KBr, cm⁻¹): 3432 (NH imidazole), 3047 (C–H aromatic), 1784, 1723 (C=O imide), 1600 (C=N imidazole), 1497 (C=C), 1368 (C–N) and 1254 (C–O). ¹H NMR (DMSO-*d*₆): δ 1.32 (t, 3H, CH₃), 4.44 (q, 2H, CH₂), 7.11–8.65 (m, 27H, Ar-H), 12.66 (s, 1H, N–H imidazole ring). Anal. Calcd. (%) for $(C_{61}H_{33}F_{12}N_5O_6)_n$: C, 63.16; H, 2.85; N, 6.04. Found: C, 63.02; H, 2.96; N, 6.01.

4.6. Preparation of electrode

The PEIIs containing imidazol-derivative is electrochemical active and insoluble in aqueous solutions, thus it can be simply

incorporated into the carbon paste without concern regarding its leaching from the electrode surface. For the electrochemical investigation, a mixture of 10 mg polymer with 80 mg graphite powder and 10 mg carbon nanotubes was prepared in a mortar and pestle. Then using a syringe, 0.75 g paraffin was added to the mixture and mixed well for 70 min until a uniformly wetted paste was obtained. The paste was then packed into a glass tube. Electrical contact was made by pushing a copper wire down the glass tube into the back of the mixture. When necessary, a new surface was obtained by pushing an excess of the paste out of the tube and polishing it on a weighing paper.

4.7. Stability and reproducibility

The repeatability and stability of the polymer in CNTs paste matrix was investigated by cyclic voltammetry measurements. The relative standard deviation (RSD%) for five successive assays is 2.8%. When using four different electrodes, the RSD% for five measurements is 3.5%. When stored in a laboratory, the modified electrode retains 97% of its initial response after a week and 94% after 30 days.

Acknowledgments

We wish to express our gratitude to the Research Affairs Division of University of Mazandaran (UMZ), Babolsar (Iran), for partial financial support.

References

- [1] P. Wasserscheid, T. Welton, *Ionic Liquids in Synthesis*, Wiley-VCH Verlag GmbH & Co. KGaA, 2002 (Edited by Copyright).
- [2] J. Lu, F. Yan, J. Texter, *Progress in Polymer Science* 34 (2009) 431–448.
- [3] K. Przemyslaw, *Progress in Polymer Science* 29 (2004) 3–12.
- [4] T. Welton, *Chemical Reviews* 99 (1999) 2071–2084.
- [5] E.I. Lozinskaya, A.S. Shaplov, Y.S. Vygodskii, *European Polymer Journal* 40 (2004) 2065–2075.
- [6] P. Kubisa, *Journal of Polymer Science. Part A: Polymer Chemistry* 43 (2005) 4675–4683.
- [7] E.I. Lozinskaya, A.S. Shaplov, M.V. Kotseruba, L.I. Komarova, K.A. Lyssenko, M.Y. Antipin, *Journal of Polymer Science. Part A: Polymer Chemistry* 44 (2006) 380–394.
- [8] M. Yoneyama, *High Performance Polymers* 18 (2006) 817–823.
- [9] J.P. Paraknowitsch, A. Thomas, M.A. Antonietti, *Journal of Materials Chemistry* 20 (2010) 6746–6758.
- [10] Y.S. Vygodskii, L.E.I. ozinskaya, A.S. Shaplov, K.A. Lyssenko, M.Y. Antipin, Y.G. Urman, *Polymer Journal* 45 (2004) 5031–5045.
- [11] D. Wilson, H.D. Stenzenberger, P.M. Hergenrother, *Polyimides*, Chapman and Hall, New York, 1990.
- [12] M.K. Ghosh, K.L. Mittal, *Polyimides Fundamentals and Applications*, Marcel Dekker, New York, 1996.
- [13] G. Maier, *Progress in Polymer Science* 26 (2001) 3–65.
- [14] Y. Shao, Y. Li, X. Zhao, T. Ma, C. Gong, F. Yang, *European Polymer Journal* 43 (2007) 4389–4397.
- [15] J.G. Liu, M.H. He, Z.G. Ian, S.Y. Yang, *Journal of Polymer Science. Part A: Polymer Chemistry* 40 (2002) 1572–1582.
- [16] S.M. Amini Nasab, M. Ghaemy, *Journal of Polymer Research* 18 (2011) 1575–1586.
- [17] M. Ghaemy, M. Barghamadi, *Journal of Applied Polymer Science* 112 (2009) 815–821.
- [18] S. Mehdipour-Ataei, N. Bahri-Laleh, A. Amirshaghghi, *Polymer Degradation and Stability* 91 (2006) 2622–2631.
- [19] X.-L. Wang, Y.-F. Li, C.-L. Gong, T. Ma, F.-C. Yang, *Journal of Fluorine Chemistry* 129 (2008) 56–63.
- [20] M. Ghaemy, M. Bazzar, *Journal of Applied Polymer Science* 119 (2011) 983–988.
- [21] Y.U. Bae, T.H. Yoon, *Journal of Applied Polymer Science* 123 (2012) 3298–3308.
- [22] G.S. Liou, S.H. Hsiao, N.K. Huang, Y.L. Yang, *Macromolecules* 39 (2006) 5337–5346.
- [23] M. Ghaemy, S.M. Amini Nasab, *Polymer Journal* 42 (2010) 648–656.
- [24] M. Ghaemy, R. Alizadeh, *European Polymer Journal* 45 (2009) 1681–1688.
- [25] F. Yang, Y. Li, T. Ma, Q. Bu, S. Zhang, *Journal of Fluorine Chemistry* 131 (2010) 767–775.
- [26] T. Ma, S. Zhang, Y. Li, F. Yang, C. Gong, J. Zhao, *Journal of Fluorine Chemistry* 131 (2010) 724–730.
- [27] X.-J. Zhao, J.-G. Liu, H.-S. Li, L. Fan, S.-Y. Yang, *Journal of Applied Polymer Science* 111 (2009) 2210–2219.
- [28] S. Iijima, *Nature* 354 (1991) 56–58.
- [29] D. Tasis, N. Tagmatarchis, A. Bianco, M. Prato, *Chemical Reviews* 106 (2006) 1105–1136.
- [30] R.L. McCreery, *Chemical Reviews* 108 (2008) 2646–2687.
- [31] S. Mallakpour, M. Taghavi, *Polymer* 49 (2008) 3239–3249.
- [32] Q. Mi, Z. Wang, C. Chai, J. Zhang, B. Zhao, C. Chen, *Microchimica Acta* 173 (2011) 459–467.
- [33] Y.S. Vygodskii, E.I. Lozinskaya, A.S. Shaplov, *Macromolecular Rapid Communications* 23 (2002) 676–680.
- [34] G.S. Liou, C.W. Chang, *Macromolecules* 41 (2008) 1667–1674.
- [35] H. Behniafar, S. Khosravi-bornia, *Polymer International* 58 (2009) 1299–1307.
- [36] D.W. Van Krevelen, *Properties of Polymers*, fourth ed., Elsevier Scientific Publishing, 2008.
- [37] C.-L. Chung, W.-F. Lee, C.-H. Lin, S.-H. Hsiao, *Journal of Polymer Science. Part A: Polymer Chemistry* 47 (2009) 1756–1770.
- [38] S. Sheng, D. Li, T. Lai, X. Liu, C. Song, *Polymer International* 60 (2011) 1185–1193.
- [39] M. Ghaemy, S.M. Amini Nasab, *Reactive and Functional Polymers* 70 (2010) 306–311.
- [40] A.A. Ensafi, H. Karimi-Maleh, *Journal of Electroanalytical Chemistry* 640 (2010) 75–83.
- [41] S. Mallakpour, M. Hatami, A.A. Ensafi, H. Karimi-Maleh, *Journal of Solid State Electrochemistry* 15 (2011) 2053–2061.